IEEE Access
Multidisciplinary ⋮ Rapid Review ⋮ Open Access Journal

Received 5 May 2024, accepted 8 June 2024, date of publication 11 June 2024, date of current version 20 June 2024.

Digital Object Identifier 10.1109/ACCESS.2024.3412816

RESEARCH ARTICLE

Three-Dimensional Path Following Control of Underactuated AUV Based on Nonlinear Disturbance Observer and Adaptive Line-of-Sight Guidance

LONG HE, YA ZHANG, GANG FAN, YANG LIU, XUE WANG, AND ZEHUI YUAN
College of Mechatronic Engineering, North University of China, Taiyuan 030051, China

Corresponding author: Ya Zhang (hlonghb@163.com)

This work was supported in part by the Weapons and Equipment Advance Research Project of the Central Military Commission under Grant 90903010102, in part by the 19th Graduate Science and Technology Project of the North University of China under Grant 20231903, and in part by the Fundamental Research Program of Shanxi Province under Grant 202303021212190.

ABSTRACT In this study, a backstepping sliding mode control method (NDO-ABSC) based on nonlinear disturbance observer (NDO) and adaptive line-of-sight guidance (ALOS) is proposed to address the three-dimensional path following control problem of underactuated autonomous underwater vehicles (AUVs) in the presence of ocean currents, unmodeled dynamics, and other unknown disturbances. First, the following error equations in the current environment are established in the Serret-Frenet coordinate system. Then, ALOS is designed to estimate the variations changes in angle-of-attack and crab angle caused by time-varying currents. In the kinematic controller, a parameter adaptive law, a control law for the virtual target point, and a virtual desired angular velocity are designed by backstepping. Subsequently, the composite uncertainty disturbance is observed and compensated by constructing a nonlinear disturbance observer, and a dynamic controller is designed by backstepping method, and a sliding mode control term is introduced in the control law to enhance the robustness of the system to the uncertainty disturbance. Finally, the good performance and strong robustness of the proposed method in 3D path following control are verified by numerical simulation.

INDEX TERMS AUV, path following, nonlinear disturbance observer, adaptive line of sight, backstepping.

I. INTRODUCTION

Unmanned underwater vehicles (UUVs) play a crucial role in tasks such as seabed mapping, resource exploration, environmental monitoring, and underwater mine clearance, making them vital assets for ocean exploration and development [1], [2], [3]. Among them, underactuated AUVs need to have good path following capability to effectively accomplish these tasks. Due to the effects of time-varying currents, waves, and other unknown disturbances, the spatial motion model of an AUV is a complex nonlinear coupled system, which also includes uncertainties in the model's own parameters, which increases the difficulty of path following controller design [4]. However, it has also aroused extensive research interest from many scholars, and different approaches have been studied and focused on.

The guidance law is one of the keys to solve the underactuated AUV path following problem. Among the traditional path following methods, the line-of-sight (LOS) guidance law is commonly used to realize path following by generating a reference trajectory with yaw angle [5], [6], [7]. However, in complex environments such as currents, where unknown drift forces affect the motion of the navigator, the traditional LOS method is difficult to cope with this challenge and may lead to large trajectory errors. In addition, many other studies have mentioned several methods for path following in the presence of currents, including integral line-of-sight (ILOS) guidance, adaptive ILOS guidance,

The associate editor coordinating the review of this manuscript and approving it for publication was Wonhee Kim.

extended state observer-based line-of-sight (ELOS) guidance, and adaptive line-of-sight (ALOS) guidance.The ILOS guidance adds an integral term to the traditional LOS guidance law to reduce the unknown effects of drift forces and improves the path following performance [8], [9], [10], [11], adaptive ILOS guidance uses the unknown crab angle as a constant parameter, estimates it using an adaptive law, and introduces an inverse tangent function to compensate for the sideslip [12], [13], and the ELOS method utilizes an extended state observer to estimate the perturbations caused by ocean currents so that the unmeasured crab angle can be indirectly computed and compensated accurately [14], [15], [16]. To better follow the curved path, a forward-looking distance adjustment scheme that can adapt to the changing situation is given in [17] and [18]. Although these methods mitigate the effect of unknown drift forces to some extent, the above methods still have some limitations for rapidly changing crab angles subject to time-varying current perturbations. In 2023, Fossen proposed an adaptive line-of-sight (ALOS) guidance law and conducted a simulation study in the horizontal plane, which verified that the guidance law has a better following ability in compensating for the rapidly changing sideslip caused by time-varying perturbations [19]. Drawing on the ideas of the previous literature, an adaptive line-of-sight method is proposed to compensate for the crab angle and the angle of attack. Unlike the adaptive ILOS guidance method, we introduce the angle estimation outside the inverse tangent function, which is able to deal with the rapid angle change caused by the sea current effectively. In order to better follow the curved path, a forward-looking distance that can be flexibly adjusted is designed, and compared with the previous methods, the proposed method has better adaptability and estimation capability.

Underactuated AUVs face a variety of uncertainties in real-world navigation, including uncertainties in model hydrodynamic parameters, unknown environmental disturbances, and unmodeled dynamic properties. These uncertainties and disturbances may lead to degradation of the system control quality or even system instability. In this paper, we deal with these uncertainties and disturbances by designing a nonlinear disturbance observer and introducing the idea of sliding mode control to improve the control accuracy and stability of the AUV. Several approaches have been used to solve these problems as well. In [20] and [21], the authors used a fuzzy mechanism to estimate the uncertainty term, but the merit of the fuzzy rules affects the approximation error. In [22], the system stability in finite time is ensured by adaptive anti-disturbance law and fast terminal sliding mode control considering the parameter uptake and uncertain disturbances. In [23] and [24], a fractional-order sliding-mode disturbance observer (FOSMDO) is designed to provide an effective estimation of random disturbances in the environment, and a sliding-mode control strategy is used to ensure the following accuracy. In [25], [26], and [27], the impact of the disturbances on the system was mitigated by estimating the aggregate disturbances through a disturbance observer. Considering the upper limit of the observation error of the observer as a constant may affect the dynamic performance of the system when there is a large change in the external disturbance. Therefore, when designing the disturbance observer, we introduce an adaptive mechanism to estimate the upper limit of the observation error online in order to better adapt to changes in the external environment.

In the control strategy design of AUVs, the control tasks are often decomposed into two-dimensional planar path following and one-dimensional depth control, which simplifies the complexity of the system design and allows the controllers to focus on their respective tasks, which effectively improves the performance and robustness of the system. However, for certain application scenarios [28], [29], [30], [31], such as maneuvering dives under 3D spiral paths, navigating in narrow and obstacle-ridden waters, or inspecting submarine pipelines, AUVs are required to perform more complex 3D motions. In particular, when monitoring offshore oil pipeline rack platforms, AUVs need to adopt 3D spiral motion patterns, in which traditional decoupled control designs may not be able to achieve the desired path following effect. In the pipeline inspection mission, due to the possible presence of sediments near the pipeline, the AUV must have accurate 3D obstacle avoidance capability. In addition, in military missions such as underwater confrontation, the vehicle needs to avoid obstacles while navigating normally, which also requires the AUV to be able to perform complex 3D maneuvers. The direct design of a controller capable of following 3D paths allows for the simultaneous consideration of horizontal and vertical path tracking within a unified control framework, which improves the efficiency and accuracy of mission execution.

For those AUVs performing tasks in open water, traditional decoupled control methods may be sufficient. However, when the AUV is in narrow or obstacle-laden waters, or performing tasks such as military, more sophisticated 3D curved path following techniques are required. Several studies have proposed different solutions for 3D path following control of underactuated AUVs. First, Do et al. proposed a control strategy for underactuated AUVs, which is capable of efficiently tracking along a predetermined path following unknown physical parameters and environmental disturbances, but may face the challenges of model accuracy and practical validation [33].Breivik proposed a single controller structure, which is capable of solving the 3D path following of AUVs at different speeds, but may face the complexity of controller design [32].The control strategy proposed by Aguiar, on the other hand, is independent of path type and can track any sufficiently smooth bounded curves, but its adaptability to parameter uncertainty still needs to be improved in practical applications [34].Fischer et al. validated their control strategy in both a control pool and an open-water environment, and obtained, under system uncertainty and external perturbations good tracking results, and the adaptability to actuator

dynamics and marine environment may need further improvement [35].Peymani et al. used a Lagrange multiplier-based approach to design a path following controller to solve the 3-dimensional path following problem in the case of saturated thrusters, which may be affected by the computational complexity and the dynamics of marine environment [30]. In addition, Xiang et al. proposed a new control framework applicable to AUVs tracking 3D tanh paths and elliptical paths, which solves the path tracking problem of underactuated AUVs in 3D space, but may depend on fuzzy logic parameter tuning [28].Zhang et al. proposed a control scheme applicable to AUVs tracking parameterized paths in 3D space, which solves the path tracking problem of AUVs in un modeling dynamics, actuator lag, and ocean perturbations, and other multiple uncertainties and nonlinearities, but the complexity of control parameter tuning and validation in real ocean environments are issues that need to be considered [29]. Based on these studies, multiple control methods and improved estimation methods are synthesized to address the challenges of AUV path following in marine environments. Angle estimation and the design of a nonlinear disturbance observer are introduced to effectively improve the system's resistance to uncertainties and external perturbations. Meanwhile, the introduced sliding mode control term further enhances the robustness of the system.

Inspired by the above literature, a backstepping sliding mode control method (NDO-ABSC) based on a nonlinear disturbance observer and adaptive line-of-sight guidance is proposed to solve the problem of underactuated AUV 3D path following control in the presence of multiple uncertainties, such as currents and other unknown disturbances. The main contributions of this paper are as follows:

1) A nonlinear disturbance observer is designed to estimate the composite uncertainty disturbance term consisting of parameter uncertainty and external disturbance, etc. Meanwhile, an adaptive law is introduced to estimate the upper term of the observation error online to improve the following performance and robustness of the system.

(2) An adaptive line-of-sight guidance law is designed to compensate for the drift force caused by time-varying currents, and an adaptive forward-looking distance is designed to track the curved path following better than the traditional LOS.

3) The 3D path following error and its dynamical equations of an underactuated AUV in a current environment are derived, and a sliding mode control term is introduced in the last step of the backstepping controller design to compensate for the unobserved part of the uncertainty disturbances and to improve the robustness of the system.

The rest of the section is organized as follows: the mathematical model and error equations of the underactuated AUV are described in Section II. The design process of the kinematics and dynamics controllers and the stability analysis of the system are given in Section III. Results and discussion of numerical simulations are given in Section IV. Section V is the conclusion section.

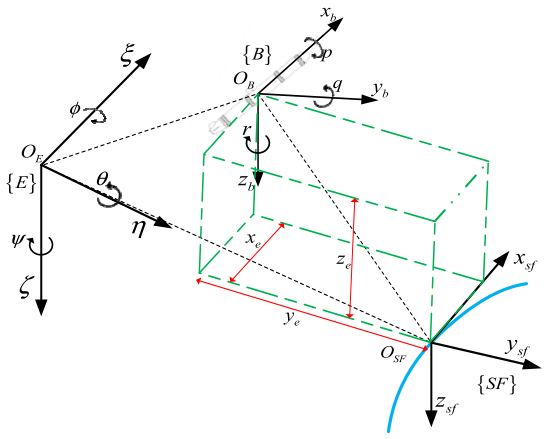

FIGURE 1. Schematic diagram of 3D path following.

II. AUV MODEL AND PROBLEM DESCRIPTION

In this section, the following error and its dynamics model of an underactuated AUV moving in 3D space in a current environment are derived and the 3D path following motion control problem is described. First, the airframe coordinate system and geodesic coordinate system are established, and the corresponding symbols and conventions are defined. Then, the kinematic and dynamic models of the underactuated AUV are given. Next, the following error model is derived to describe the path following control problem of an underactuated AUV in 3D space.

A. MATHEMATICAL MODELING OF AUVS UNDER THE INFLUENCE OF CURRENTS

In order to describe the spatial motion of the AUV, two coordinate systems are defined, namely the body coordinate system$\{B\} : O_B - x_b y_b z_b$ and the geodetic coordinate system$\{E\} : O_E - \xi\eta\zeta$. The origin O_B of the body coordinate system is at the floating center of the AUV, the axes are established in accordance with the rules of the right-handed coordinate system, and all the symbols are adopted from the symbols recommended by the International Towed Tank Conference (ITTC). The specific definitions are shown in Fig. 1. The kinematics and dynamics of the AUV are modeled as:

$$\dot{\eta} = J(\eta)\, v_r + v_f \tag{1}$$

$$M\dot{v}_r + C(v_r)\, v_r + D(v_r)\, v_r + g(\eta) = \tau + \tau_d \tag{2}$$

where,$\eta = [x\ y\ z\ \phi\theta\psi]^{\mathrm{T}}$, x, y, z is the coordinate of the origin of the body coordinate system in the geodetic coordinate system, which represents the global position of the AUV, and ϕ, θ, ψ is the three Euler angles between the geodetic coordinate system and the body coordinate system, which represents the attitude of the AUV. $J(\eta)$ is the transformation matrix from $\{B\}$ to $\{E\}$. $v_r = [u_r v_r w_r p\ qr]^{\mathrm{T}}$ is the velocity vector of the AUV relative to the water flow, i.e. $v_r = v - v_c$, where $v = [uv\ wp\ qr]^{\mathrm{T}}$ is the absolute velocity vector of the AUV in the body coordinate system, and $v_c = \left[u_{cx} v_{cy} w_{cz} 0\ 0\ 0\right]^{\mathrm{T}} = J^{\mathrm{T}}(\eta)\, v_f$ is the velocity vector of the water flow in the body

coordinate system. M is the inertia matrix, $C(v_r)$ is the Götter force and centripetal force matrix, and $D(v_r)$ is the damping matrix. $g(\eta) = \left[0\ 0\ 0\ 0\ M_g\ 0\right]^{\mathrm{T}}$ is the gravity and buoyancy restoring force matrix. $\tau = [X_\tau\ 0\ 0\ 0\ M_\tau\ N_\tau]^{\mathrm{T}}$ is the control input vector of the AUV. τ_d is the disturbance vector consisting of uncertainties in the model parameters and unknown environmental disturbances.

Assuming that the AUV prototype studied in the paper has a uniformly distributed body mass, with gravity balanced by buoyancy, and the center of buoyancy is located in the vertical plane, and the transverse rocking motion is neglected. In order to show the relationship between the state variables of the AUV more intuitively and to facilitate the design of the controller, equation (1) and (2) are simplified to the following set of kinematic and dynamic equations:

$$\begin{cases} \dot{x} = u_r\cos\psi\cos\theta - v_r\sin\psi + w_r\cos\psi\sin\theta + u_{f\xi} \\ \dot{y} = u_r\sin\psi\cos\theta + v_r\cos\psi + w_r\sin\psi\sin\theta + v_{f\eta} \\ \dot{z} = -u_r\sin\theta + w_r\cos\theta + w_{f\zeta} \\ \dot{\theta} = q \\ \dot{\psi} = r/\cos\theta \end{cases} \tag{3}$$

$$\begin{cases} \dot{u}_r = \dfrac{m_2}{m_1}v_r r - \dfrac{m_3}{m_1}w_r q - \dfrac{d_1}{m_1}u_r + \dfrac{1}{m_1}X_r + \tau_{du} \\ \dot{v}_r = -\dfrac{m}{m_2}z_g rq - \dfrac{m_1}{m_2}u_r r - \dfrac{d_2}{m_2}v_r + \tau_{dv} \\ \dot{w}_r = \dfrac{m}{m_3}z_g q^2 + \dfrac{m_1}{m_3}u_r q - \dfrac{d_3}{m_3}w_r + \tau_{dw} \\ \dot{q} = -\dfrac{m_1 - m_3}{m_4}u_r w_r + \dfrac{m}{m_4}z_g\left(rv_r - qw_r\right) - \dfrac{d_4}{m_4}q - M_g \\ +\dfrac{1}{m_4}M_\tau + \tau_{dq} \\ \dot{r} = \dfrac{m_1 - m_2}{m_5}u_r v_r - \dfrac{d_5}{m_5}r + \dfrac{1}{m_5}N_r + \tau_{dr} \end{cases} \tag{4}$$

where,

$$\begin{aligned} &m_1 = m - X_{\dot{u}},\ m_2 = m - Y_{\dot{v}},\ m_3 = m - Z_{\dot{w}},\ m_4 = I_{yy} - M_{\dot{q}}, \\ &\quad m_5 = I_{zz} - N_{\dot{r}},\ m_g = z_g G\sin\theta \\ &d_1 = -X_u - X_{u|u|}|u|,\ d_2 = -Y_v - Y_{v|v|}|v| \\ &d_3 = -Z_w - Z_{w|w|}|w|,\ d_4 = -M_q - M_{q|q|}|\,q| \\ &d_5 = -N_r - N_{r|r|}|r| \end{aligned}$$

m is the mass of the AUV, I_{yy} and I_{zz} are the moment of inertia of the AUV, G denote the gravity forces on the AUV, $d_{(\cdot)}$ is the nonlinear damping term, $X_{(\cdot)}$, $Y_{(\cdot)}$, $Z_{(\cdot)}$, $M_{(\cdot)}$, $N_{(\cdot)}$ are the coefficient of hydrodynamics of the viscous fluid, and z_g is the position of the center of gravity on the vertical axis in the body coordinates.

B. 3D PATH FOLLOWING ERROR MODELING

In Fig. 1, $\{E\}$ and $\{B\}$ denote the geodetic coordinate system and the body coordinate systems respectively, in order to establish the following error model, $\{E\}$ is rotated around the

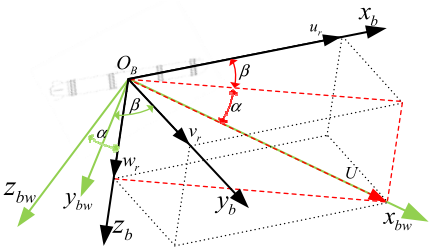

FIGURE 2. Coordinate system conversion.

$O_E\zeta$-axis and the $O_E\eta$-axis respectively, with the rotation angles of ψ_f and θ_f, in order to define the path coordinate system $\{SF\}: O_{SF} - x_{sf}y_{sf}z_{sf}$, the origin of the $\{SF\}$ is the reference point of the path following, and its position under the $\{E\}$ is denoted by $\eta_{d1} = [x_d(s)\, y_d(s)\, z_d(s)]^{\mathrm{T}}$, and the rotation angle is denoted by $\eta_{d2} = \left[\theta_f\, \psi_f\right]^{\mathrm{T}}$, as specified in:

$$\begin{cases} \theta_f = -\arctan\left(\dfrac{z_d'(s)}{\sqrt{\left(x_d'(s)\right)^2 + \left(y_d'(s)\right)^2}}\right) \\ \psi_f = \mathrm{a\,tan\,2}\left(y_d'(s), x_d'(s)\right) \end{cases} \tag{5}$$

where, $x_d' = \partial x_d/\partial s, y_d' = \partial y_d/\partial s$, s is the arc length parameter of the desired path curve, then the forward velocity of the virtual target O_{SF} is denoted by $u_F = \dot{s}$.

c_t and c_u are the deflection and curvature of the path curve, and the rotation angular rate can be expressed as:

$$\begin{cases} \dot{\theta}_f = c_t\dot{s} \\ \dot{\psi}_f = c_u\dot{s} \end{cases} \tag{6}$$

The disturbance of the current will cause the lateral and vertical velocity of the AUV to change continuously, and the influence of the angle of attack and crab angle on navigation will not be negligible. In order to facilitate the subsequent calculations, a new coordinate system $\{W\}: O_B - x_{bw}y_{bw}z_{bw}$ is introduced, and the body coordinate system is rotated around the O_Bz-axis and the O_By-axis respectively, with the rotation angles of β and α, and the direction of the AUV's merging velocity U is taken as the longitudinal axis, as shown in Fig. 2.Based on the $\{W\}$, the position of the AUV in the $\{E\}$ is denoted by $\eta_1 = [x\ y\ z]^{\mathrm{T}}$. The attitude angle is denoted by $\eta_2 = [\theta + \alpha\ \psi + \beta]^{\mathrm{T}}$, where:

$$\begin{cases} \alpha = -\arctan\left(\frac{w}{u}\right) \\ \beta = \arctan\left(\frac{v}{u}\right) \end{cases} \tag{7}$$

Define the position error $P_e = [x_e\ y_e z_e]^{\mathrm{T}} = R_1(\eta_1 - \eta_{d1})$, attitude error $A_e = [\theta_e\psi_e]^{\mathrm{T}} = R_2(\eta_2 - \eta_{d2}) = [\theta + \alpha - \theta_f\frac{\psi+\beta-\psi_f}{\cos\theta_f}]^{\mathrm{T}}$ in the $\{SF\}$, where R_1 and R_2 are the transformation matrix from $\{E\}$ to $\{SF\}$, i.e.

$$R_1 = \begin{bmatrix} \cos\psi_f\cos\theta_f & \sin\psi_f & -\cos\psi_f\sin\theta_f \\ -\sin\psi_f\cos\theta_f & \cos\psi_f & \sin\psi_f\sin\theta_f \\ \sin\theta_f & 0 & \cos\theta_f \end{bmatrix} \tag{8}$$

$$R_2 = \begin{bmatrix} 1 & 0 \\ 0 & \cos\theta_f \end{bmatrix} \tag{9}$$

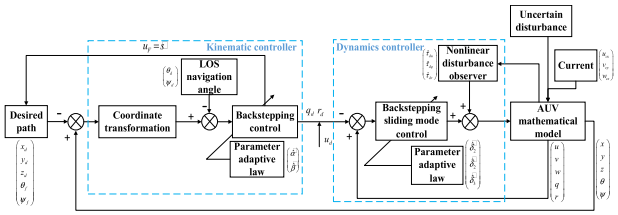

FIGURE 3. Schematic diagram of path following control.

Derivation of the position error equation, can obtaine:

$$\dot{P}_e = \begin{bmatrix} \dot{x}_e \\ \dot{y}_e \\ \dot{z}_e \end{bmatrix} = \begin{bmatrix} \dot{\psi}_f y_e - \dot{\theta}_f z_e + U\cos\psi_e \cos\theta_e - u_F \\ -\dot{\psi}_f x_e - \dot{\psi}_f \tan\theta_f z_e + U\sin\psi_e \cos\theta_e \\ \dot{\theta}_f x_e + \dot{\psi}_f \tan\theta_f y_e - U\sin\theta_e \end{bmatrix} \tag{10}$$

The 3D path following control problem for an underactuated underwater vehicle can be described as follows: given a predefined bounded 3D path $\eta_{d1} = [x_d(s)\, y_d(s)\, z_d(s)]^{\mathrm{T}}$, design a robust control law X_τ, M_τ, N_τ based on the mathematical models (3) and (4), taking into account factors such as currents, uncertainties in the AUV model parameters, and other unknown environmental disturbances. The goal of this control law is to make the body coordinate origin asymptotically converge to the virtual target point, and move along the spatial path, given the desired forward velocity, while keeping the combined velocity aligned with the tangent vector of the path [29].

III. 3D PATH FOLLOWING CONTROLLER DESIGN

The design of the controller is divided into two main steps: the first step is based on the ALOS guidance to compensate the drift and lift due to unknown currents. In this step, the backstepping method is used to design the control law for the virtual target point and the virtual desired angular velocity, and the parametric adaptive law is obtained to complete the design of the kinematic controller. In the second step, a nonlinear disturbance observer is proposed to estimate the composite uncertain disturbances, including external disturbances, parameter uncertainties and modeling errors. In this step, an adaptive approach is used to estimate the upper bound of the observation error online. Subsequently, the desired angular velocity derived in the previous step is used as the reference signal, the desired forward velocity is introduced, and a sliding mode control term is added in the last step of the backstepping method, so as to obtain the control law of the force and torque, and the design of the dynamics controller is completed. The structure of the whole control system is shown in Fig. 3.

A. KINEMATIC CONTROLLER DESIGN

For underactuated AUVs, due to their lack of lateral and vertical propulsion, in order to reduce the following error, the LOS method is usually used to introduce the navigation angle, which simulates an experienced helmsman to convert the position error into the azimuth error [36]. For the drift and lift caused by currents, the ALOS guidance law is proposed to compensate in order to reduce its effect on path following. Instead of the integral term added to the function in the traditional ILOS guidance law [8], [9], [10], [11], [12], [13], an estimate is introduced outside the inverse tangent function, which makes the derivation of the formula relatively simpler. The desired navigation angle given by the ALOS guidance law is expressed as:

$$\begin{cases} \theta_d = \theta_f + \arctan\left(\frac{z_e}{\Delta_\theta}\right) + \hat{\alpha} \\ \psi_d = \psi_f - \arctan\left(\frac{y_e}{\Delta_\psi}\right) - \hat{\beta} \end{cases} \tag{11}$$

where: $\hat{\alpha}$, $\hat{\beta}$ are the estimated values of angle of attack and crab angle, and Δ_θ and Δ_ψ are the forward-looking distances.

In the traditional LOS method, the forward-looking distance is usually regarded as a constant and is mainly used for simple linear following. However, the following performance of this method is poor when considering path following complex curves in unknown environments. In order to better adapt to path variations, a saturation function sat $(\cdot)$, which describes the forward-looking distance as a function of the deflection and curvature, is introduced as:

$$\begin{cases} \Delta_\theta = l\left(2.5 - \mathrm{sat}(k_{ct}\frac{c_t}{c_{t\max}})\right) \\ \Delta_\psi = l\left(2.5 - \mathrm{sat}(k_{cu}\frac{c_u}{c_{u\max}})\right) \end{cases} \tag{12}$$

where: k_{ct}, k_{cu} are the scale factors used to adjust the transformation trend, l is the length of the AUV.

Let $\theta = \theta_d$, $\psi = \psi_d$, substituting equation (11) into equation (10), can get:

$$\begin{bmatrix} \dot{x}_e \\ \dot{y}_e \\ \dot{z}_e \end{bmatrix} = \begin{bmatrix} \dot{\psi}_f y_e - \dot{\theta}_f z_e + U\cos\psi_e\cos\theta_e - u_F \\ -\dot{\psi}_f x_e - \dot{\psi}_f \tan\theta_f z_e + U\sin\left(\frac{\psi_d+\beta-\psi_f}{\cos\theta_f}\right)\cos\theta_e \\ \dot{\theta}_f x_e + \dot{\psi}_f \tan\theta_f y_e - U\sin\left(\theta_d + \alpha - \theta_f\right) \end{bmatrix} \tag{13}$$

Define the error variables $\tilde{\theta} = \theta - \theta_d$, $\tilde{\psi} = \psi - \psi_d$, $\tilde{\alpha} = \alpha - \hat{\alpha}$, $\tilde{\beta} = \beta - \hat{\beta}$, let $U = k_b U_r$, constructs the Lyapunov function $V_1 = \frac{1}{2}P_e^{\mathrm{T}}P_e + \frac{k_b U_r}{2k_\alpha}\tilde{\alpha}^2 + \frac{k_b U_r}{2k_\beta}\tilde{\beta}^2 + \frac{1}{2}\tilde{\theta}^2 + \frac{1}{2}\tilde{\psi}^2$, because $\tilde{\alpha}$ and $\tilde{\beta}$are smaller, so there are $\cos\tilde{\alpha} \approx 1$, $\cos\tilde{\beta} \approx 1 \sin\tilde{\alpha} \approx \tilde{\alpha}$, $\sin\tilde{\beta} \approx \tilde{\beta}$, the derivation of V_1 can be obtained as follows.

$$\begin{aligned} \dot{V}_1 &= x_e\dot{x}_e + y_e\dot{y}_e + z_e\dot{z}_e - \frac{k_b U_r}{k_\alpha}\tilde{\alpha}\dot{\tilde{\alpha}} - \frac{k_b U_r}{k_\beta}\tilde{\beta}\dot{\tilde{\beta}} + \tilde{\theta}\dot{\tilde{\theta}} + \tilde{\psi}\dot{\tilde{\psi}} \\ &= x_e\left(k_b U_r\cos\psi_e\cos\theta_e - u_F\right) - \frac{k_b U_r z_e^2}{\sqrt{\Delta_\theta^2 + z_e^2}} \\ &\quad - \tilde{\alpha}\left(\frac{k_b U_r z_e \Delta_\theta}{\sqrt{\Delta_\theta^2 + z_e^2}} - \frac{k_b U_r}{k_\alpha}\dot{\hat{\alpha}}\right) - \frac{k_b U_r y_e^2\cos\theta_e}{\sqrt{\Delta_\psi^2 + y_e^2}} \\ &\quad + \tilde{\beta}\left(\frac{k_b U_r y_e \Delta_\psi\cos\theta_e}{\sqrt{\Delta_\psi^2 + y_e^2}} - \frac{k_b U_r}{k_\beta}\dot{\hat{\beta}}\right) + \tilde{\theta}\left(q - \dot{\theta}_d\right) \\ &\quad + \tilde{\psi}\left(\frac{r}{\cos\theta} - \dot{\psi}_d\right) \end{aligned} \tag{14}$$

Design the velocity control law of the virtual target point and the virtual angular velocity control law as:

$$\begin{cases} u_F = k_b U_r \cos\psi_e \cos\theta_e + k_1 x_e \\ q_d = -k_\theta \tilde{\theta} + \dot{\theta}_d \\ r_d = \cos\theta(-k_\psi \tilde{\psi} + \dot{\psi}_d) \end{cases} \tag{15}$$

where k_b, k_1, k_θ, k_ψ are scale factors, all greater than zero. And the parameter adaptive law is:

$$\begin{cases} \dot{\hat{\alpha}} = \frac{k_\alpha z_e \Delta_\theta}{\sqrt{\Delta_\theta^2 + z_e^2}} \\ \dot{\hat{\beta}} = \frac{k_\beta y_e \Delta_\psi \cos\theta_e}{\sqrt{\Delta_\psi^2 + y_e^2}} \end{cases} \tag{16}$$

where k_α, k_β are the adaptive gain.

Substituting equation (15) and (16) into equation (14), can obtain:

$$\begin{aligned} \dot{V}_1 = &-k_1 x_e^2 - \frac{k_b U_r z_e^2}{\sqrt{\Delta_\theta^2 + z_e^2}} - \frac{k_b U_r y_e^2 \cos\theta_e}{\sqrt{\Delta_\theta^2 + z_e^2}} \\ &- k_\theta \tilde{\theta}^2 - k_\psi \tilde{\psi}^2 \le 0 \end{aligned} \tag{17}$$

According to the Barbalat lemma, can get $\lim_{t\to\infty} \dot{V}_1 = 0 \Rightarrow \lim_{t\to\infty} \left(x_e, y_e, z_e, \tilde{\alpha}, \tilde{\beta}, \tilde{\theta}, \tilde{\psi}\right)^{\mathrm{T}} = (0,0,0,0,0,0,0)^{\mathrm{T}}$, i.e., $\lim_{t\to\infty} \alpha = \lim_{t\to\infty} \hat{\alpha}$, $\lim_{t\to\infty} \beta = \lim_{t\to\infty} \hat{\beta}$.

B. DYNAMICS CONTROLLER DESIGN

For an uncertain nonlinear system: $\dot{x} = f(x) + g(x)u + \Psi(t,x)$, where $x \in R^n$ is the system state vector, $u \in R^m$ is the control input to the system, $f(x)$ and $g(x)$are a sufficiently smooth function and satisfies the local Lipschitz condition, and $\Psi(t,x) = \Delta f(x) + \Delta g(x)u + d(t)$ is a composite disturbance consisting of uncertainty and unknown external perturbations.

A nonlinear disturbance observer is designed to estimate the composite disturbance, which takes the form [37], [38], [39]:

$$\begin{cases} \hat{\Psi} = z + p(x) \\ \dot{z} = -h(x)z - h(x)(p(x) + f(x) + g(x)u) \end{cases} \tag{18}$$

where $\hat{\Psi}$ is the output of the nonlinear interference observer, z is the internal variable, $h(x)$ is the gain, $p(x)$ is the vector of nonlinear functions to be designed and satisfies $h(x) = \partial p(x)/\partial x$.

The observation error is defined as $e_{ndo} = \Psi - \hat{\Psi}$, and the composite disturbance is slowly varying with respect to the dynamic properties of the observer, i.e., $\dot{\Psi} = 0$. The dynamic equation of the error is:

$$\begin{aligned} \dot{e}_{ndo} &= \dot{\Psi} - \dot{\hat{\Psi}} \\ &= -\dot{z} - \dot{p}(x) \\ &= h(x)(z + p(x)) - h(x)(\dot{x} - f(x) - g(x)u) \\ &= -h(x)e_{ndo} \end{aligned} \tag{19}$$

Solving the differential equation $\dot{e}_{ndo} + h(x)e_{ndo} = 0$ yields $e_{ndo}^i(t) = e_{ndo}^i(0)e^{-h_i t}$, so the observation error e_{ndo} exponentially converges to zero.

The velocity error is:

$$\begin{cases} u_e = u_r - u_d \\ q_e = q - q_d \\ r_e = r - r_d \end{cases} \tag{20}$$

taking the derivative, can get:

$$\begin{cases} \dot{u}_e = \dot{u}_r = \frac{f_1 + X_\tau}{m_1} + \tau_{du} \\ \dot{q}_e = \dot{q} - \dot{q}_d = \frac{f_2 + M_\tau}{m_4} + \tau_{dq} - \dot{q}_d \\ \dot{r}_e = \dot{r} - \dot{r}_d = \frac{f_3 + N_\tau}{m_5} + \tau_{dr} - \dot{r}_d \end{cases} \tag{21}$$

where $f_1 = m_2 v_r r - m_3 w_r q - d_1 u_r, f_2 = -(m_1 - m_3)u_r w_r + mz_g(rv_r - qw_r) - d_4 q - m_4 M_g, f_3 = (m_1 - m_2)u_r v_r - d_5 r$. τ_{du}, τ_{dq} and τ_{dr} are composite uncertain disturbances that are estimated using a nonlinear disturbance observer.

1) STABILIZE u_e

Design a nonlinear disturbance observer of the following form:

$$\begin{cases} \hat{\tau}_{du} = z_1 + p_1 \\ \dot{z}_1 = -h_1 z_1 - h_1\left(p_1 + \frac{f_1 + X_\tau}{m_1}\right) \end{cases} \tag{22}$$

where $\hat{\tau}_{du}$ is the estimated value of τ_{du}, let $e_{ndo1} = \tau_{du} - \hat{\tau}_{du}$ is the observation error of the nonlinear disturbance observer, so $\dot{u}_e = \frac{f_1 + X_\tau}{m_1} + e_{ndo1} + \hat{\tau}_{du}$, for the convenience of the controller design, assuming that the observation error of the observer to meet the $|e_{ndo1}| \le \delta_1$, $\tilde{\delta}_1 = \delta_1 - \hat{\delta}_1$, where δ_1 is an unknown bounded positive number, $\hat{\delta}_1$ is the upper bound estimate of the observation error, relative to the dynamics of the control system changes slowly, that is, to meet the $\dot{\tilde{\delta}}_1 = \dot{\delta}_1 - \dot{\hat{\delta}}_1 = -\dot{\hat{\delta}}_1$, so as to design and introduce adaptive control. The Lyapunov function is constructed as $V_2 = V_1 + \frac{1}{2}u_e^2 + \frac{1}{2}e_{ndo1}^2 + \frac{1}{2k_{\delta 1}}\tilde{\delta}_1^2$, and the derivation of V_2 can be obtained:

$$\dot{V}_2 = \dot{V}_1 + u_e\left(\frac{f_1 + X_\tau}{m_1} + e_{ndo1} + \hat{\tau}_{du}\right) - h_1 e_{ndo1}^2 - \frac{\tilde{\delta}_1 \dot{\tilde{\delta}}_1}{k_{\delta 1}} \tag{23}$$

Design control laws and adaptive laws for:

$$\begin{cases} X_\tau = -m_1\left(\hat{\delta}_1 \mathrm{sgn}(u_e) + \hat{\tau}_{du} + k_u u_e\right) - f_1 \\ \dot{\hat{\delta}}_1 = k_{\delta 1}|u_e| \end{cases} \tag{24}$$

where k_u and $k_{\delta 1}$ are adjustment factors, both greater than zero. Bringing the control law into equation (23) yields:

$$\begin{aligned} \dot{V}_2 &= \dot{V}_1 - k_u u_e^2 - h_1 e_{ndo1}^2 + u_e\left(e_{ndo1} - \hat{\delta}_1 \mathrm{sgn}(u_e)\right) - \frac{\tilde{\delta}_1 \dot{\tilde{\delta}}_1}{k_{\delta 1}} \\ &\le \dot{V}_1 - k_u u_e^2 - h_1 e_{ndo1}^2 + \delta_1 |u_e| - \hat{\delta}_1 |u_e| - \frac{\tilde{\delta}_1 \dot{\tilde{\delta}}_1}{k_{\delta 1}} \\ &= \dot{V}_1 - k_u u_e^2 - h_1 e_{ndo1}^2 + \tilde{\delta}_1\left(|u_e| - \frac{\dot{\tilde{\delta}}_1}{k_{\delta 1}}\right) \end{aligned} \tag{25}$$

bringing the adaptive law into equation (25) yields:

$$\dot{V}_2 \le \dot{V}_1 - k_u u_e^2 - h_1 e_{ndo1}^2 \tag{26}$$

2) STABILIZE q_e

Design a nonlinear disturbance observer of the following form:

$$\begin{cases} \hat{\tau}_{dq} = z_2 + p_2 \\ \dot{z}_2 = -h_2 z_2 - h_2 \left(p_2 + \frac{f_2 + M_\tau}{m_4} \right) \end{cases} \tag{27}$$

where $\hat{\tau}_{dq}$ is the estimated value of τ_{dq}, let $e_{ndo2} = \tau_{dq} - \hat{\tau}_{dq}$ is the observation error of the nonlinear disturbance observer, so $\dot{q}_e = \frac{f_2 + M_\tau}{m_4} + e_{ndo2} + \hat{\tau}_{dq} - \dot{q}_d$, for the convenience of the controller design, assuming that the observation error of the observer to meet the $|e_{ndo2}| \leq \delta_2$, $\tilde{\delta}_2 = \delta_2 - \hat{\delta}_2$, where δ_2 is an unknown bounded positive number, $\hat{\delta}_2$ is the upper bound estimate of the observation error, relative to the dynamics of the control system changes slowly, that is, to meet the $\dot{\tilde{\delta}}_2 = \dot{\delta}_2 - \dot{\hat{\delta}}_2 = -\dot{\hat{\delta}}_2$, so as to design and introduce adaptive control. The Lyapunov function is constructed as $V_3 = V_2 + \frac{1}{2} q_e^2 + \frac{1}{2} e_{ndo2}^2 + \frac{1}{2k_{\delta 2}} \tilde{\delta}_2^2$, and the derivation of V_3 can be obtained:

$$\dot{V}_3 = \dot{V}_2 + q_e \left(\frac{f_2 + M_\tau}{m_4} + e_{ndo2} + \hat{\tau}_{dq} - \dot{q}_d \right) - \frac{\tilde{\delta}_2 \dot{\hat{\delta}}_2}{k_{\delta 2}} - h_2 e_{ndo2}^2 \tag{28}$$

Design control laws and adaptive laws for:

$$\begin{cases} M_\tau = -m_4 \left(\hat{\delta}_2 \mathrm{sgn}\,(q_e) + \hat{\tau}_{dq} - \dot{q}_d + k_q q_e \right) - f_2 \\ \dot{\hat{\delta}}_2 = k_{\delta 2} \, |q_e| \end{cases} \tag{29}$$

where k_q and $k_{\delta 2}$ are adjustment factors, both greater than zero, $\hat{\delta}_2 \mathrm{sgn}\,(q_e)$ is a sliding mode control term introduced to overcome uncertainty disturbances. Bringing the control law into equation (28) yields:

$$\begin{aligned} \dot{V}_3 &= \dot{V}_2 - k_q q_e^2 - h_2 e_{ndo2}^2 + q_e \left(e_{ndo2} - \hat{\delta}_2 \mathrm{sgn}\,(q_e) \right) - \frac{\tilde{\delta}_2 \dot{\hat{\delta}}_2}{k_{\delta 2}} \\ &\leq \dot{V}_2 - k_q q_e^2 - h_2 e_{ndo2}^2 + \delta_2 \, |q_e| - \hat{\delta}_2 \, |q_e| - \frac{\tilde{\delta}_2 \dot{\hat{\delta}}_2}{k_{\delta 2}} \\ &= \dot{V}_2 - k_q q_e^2 - h_2 e_{ndo2}^2 + \tilde{\delta}_2 \left(|q_e| - \frac{\dot{\hat{\delta}}_2}{k_{\delta 2}} \right) \end{aligned} \tag{30}$$

bringing the adaptive law into equation (30) yields:

$$\dot{V}_3 \leq \dot{V}_2 - k_q q_e^2 - h_2 e_{ndo2}^2 \tag{31}$$

3) STABILIZE r_e

Design a nonlinear disturbance observer of the following form:

$$\begin{cases} \hat{\tau}_{dr} = z_3 + p_3 \\ \dot{z}_3 = -h_3 z_3 - h_3 \left(p_3 + \frac{f_3 + N_\tau}{m_5} \right) \end{cases} \tag{32}$$

where $\hat{\tau}_{dr}$ is the estimated value of τ_{dr}, let $e_{ndo3} = \tau_{dr} - \hat{\tau}_{dr}$ is the observation error of the nonlinear disturbance observer, so $\dot{r}_e = \frac{f_3 + N_\tau}{m_5} + e_{ndo3} + \hat{\tau}_{dr} - \dot{r}_d$, for the convenience of the controller design, assuming that the observation error of the observer to meet the $|e_{ndo3}| \leq \delta_3$, $\tilde{\delta}_3 = \delta_3 - \hat{\delta}_3$, where δ_3 is an unknown bounded positive number, $\hat{\delta}_3$ is the upper bound estimate of the observation error, relative to the dynamics of the control system changes slowly, that is, to meet the $\dot{\tilde{\delta}}_3 = \dot{\delta}_3 - \dot{\hat{\delta}}_3 = -\dot{\hat{\delta}}_3$, so as to design and introduce adaptive control. The Lyapunov function is constructed as $V_4 = V_3 + \frac{1}{2} r_e^2 + \frac{1}{2} e_{ndo3}^2 + \frac{1}{2k_{\delta 3}} \tilde{\delta}_3^2$, and the derivation of V_4 can be obtained:

$$\dot{V}_4 = V_3 + r_e \left(\frac{f_3 + N_\tau}{m_5} + e_{ndo3} + \hat{\tau}_{dr} - \dot{r}_d \right) - \frac{\tilde{\delta}_3 \dot{\hat{\delta}}_3}{k_{\delta 3}} - h_3 e_{ndo3}^2 \tag{33}$$

Design control laws and adaptive laws for:

$$\begin{cases} N_\tau = -m_5 \left(\hat{\delta}_3 \mathrm{sgn}\,(r_e) + \hat{\tau}_{dr} - \dot{r}_d + k_r r_e \right) - f_3 \\ \dot{\hat{\delta}}_3 = k_{\delta 3} \, |r_e| \end{cases} \tag{34}$$

where k_r and $k_{\delta 3}$ are adjustment factors, both greater than zero, $\hat{\delta}_3 \mathrm{sgn}\,(r_e)$ is a sliding mode control term introduced to overcome uncertainty disturbances. Bringing the control law into equation (33) yields:

$$\begin{aligned} \dot{V}_4 &= \dot{V}_3 - k_r r_e^2 - h_3 e_{ndo3}^2 + r_e \left(e_{ndo3} - \hat{\delta}_3 \mathrm{sgn}\,(r_e) \right) - \frac{\tilde{\delta}_3 \dot{\hat{\delta}}_3}{k_{\delta 3}} \\ &\leq \dot{V}_3 - k_r r_e^2 - h_3 e_{ndo3}^2 + \delta_3 \, |q_e| - \hat{\delta}_3 \, |q_e| - \frac{\tilde{\delta}_3 \dot{\hat{\delta}}_3}{k_{\delta 3}} \\ &= \dot{V}_3 - k_r r_e^2 - h_3 e_{ndo3}^2 + \tilde{\delta}_3 \left(|q_e| - \frac{\dot{\hat{\delta}}_3}{k_{\delta 3}} \right) \end{aligned} \tag{35}$$

bringing the adaptive law into equation (35) yields:

$$\begin{aligned} \dot{V}_4 &\leq \dot{V}_3 - k_r r_e^2 - h_3 e_{ndo3}^2 \\ &= -k_1 x_e^2 - \frac{k_b U_r z_e^2}{\sqrt{\Delta_\theta^2 + z_e^2}} - \frac{k_b U_r y_e^2 \cos\theta_e}{\sqrt{\Delta_\theta^2 + z_e^2}} - k_\theta \tilde{\theta}^2 - k_\psi \tilde{\psi}^2 \\ &\quad - k_u u_e^2 - h_1 e_{ndo1}^2 - k_q q_e^2 - h_2 e_{ndo2}^2 - k_r r_e^2 \\ &\quad - h_3 e_{ndo3}^2 \leq 0 \end{aligned} \tag{36}$$

The defined Lyapunov function V_4 is positive definite and its derivative $\dot{V}_4$ is negative semidefinite, and according to Barbalat Lemma, it is known that $\lim_{t \to \infty} \dot{V}_4 = 0 \Rightarrow \lim_{t \to \infty} \left(x_e, y_e, z_e, \tilde{\theta}, \tilde{\psi}, u_e, q_e, r_e, e_{ndo1}, e_{ndo2}, e_{ndo3} \right)^{\mathrm{T}} = 0$, hence the following error is asymptotically stable. As time progresses, the system error tends to stabilize and eventually converge to zero, indicating that the proposed control scheme can ensure the system tracks the desired path.

IV. NUMERICAL SIMULATION AND ANALYSIS OF RESULTS

In order to verify the effectiveness and robustness of the proposed path following controller, numerical simulation experiments are conducted. The simulation parameters are based on the AUV prototype model built by the team, and its specific parameters are shown in Table 1 [40]. The appearance of the prototype is shown in Fig. 4. The path following

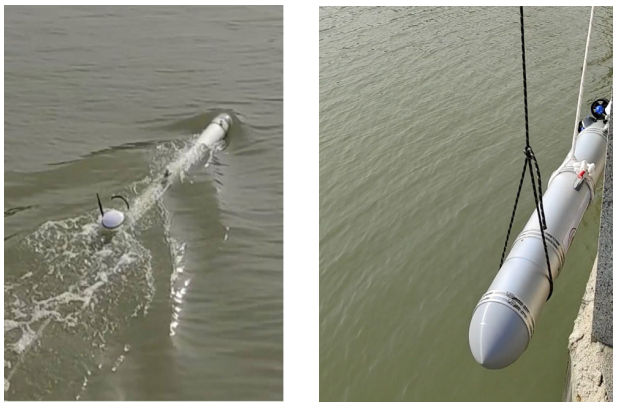

FIGURE 4. AUV prototype.

performance, disturbance estimation capability and robustness of the proposed control scheme in different environments are verified through two cases, and four methods are compared in the simulation, including:

Method I: ALOS + BS: ALOS guidance law is used for motion control and backstepping sliding mode control is used for dynamic control;

Method II: LOS + NDOBS: Conventional LOS guidance law is used for motion control and dynamic control using backstepping sliding mode control based on NDO;

Method III: ILOS + NDOBS: ILOS guidance law is used for motion control and dynamic control using backstepping sliding mode control based on NDO;

The control method proposed in this paper.

In order to analyze the performance of the system more clearly and intuitively, the mean absolute error (MAE) and root-mean-square error (RMSE) of path following are used to evaluate the following accuracy and stability. Among them, RMSE directly reflects the following stability, while MAE directly reflects the following accuracy, and these metrics will help to comprehensively evaluate the performance of different methods [18].

A. CASE 1: COMPARATIVE ANALYSIS OF PATH FOLLOWING IN CONSTANT CURRENT AND SIMPLE DISTURBANCE ENVIRONMENTS

In this case, constant currents and relatively simple disturbance conditions are selected for path following simulation. The spatial S-curve is selected as the desired path, which is parameterized as follows:

$$\begin{cases} x_d(s) = s \\ y_d(s) = 50\sin\left(\pi s/50\right) \\ z_d(s) = 0.1s \end{cases} \tag{37}$$

The initial position and attitude of the AUV is $[x(0), y(0), z(0), \theta(0), \psi(0)]^{\mathrm{T}} = [2\,\mathrm{m}, 5\mathrm{m}, 0\mathrm{m}, 0\mathrm{rad}, 0.2\mathrm{rad}]^{\mathrm{T}}$ and the initial velocity is $[u(0), v(0), w(0), q(0), r(0)]^{\mathrm{T}} = [0.15\mathrm{m/s}, 0\mathrm{m/s}, 0\,\mathrm{m/s}, 0\mathrm{rad/s}, 0\mathrm{rad/s}]^{\mathrm{T}}$. The desired forward velocity is given as 1.8m/s. The constant current is $[u_{f\xi}, v_{f\eta}, w_{f\zeta}]^{\mathrm{T}} = [0.15\mathrm{m/s}, 0.15\mathrm{m/s}, 0.1\mathrm{m/s}]^{\mathrm{T}}$, and the environmental perturbation is:

$$\begin{cases} \tau_{du} = 0.3\sin(0.3t) \\ \tau_{dq} = 0.2\sin(0.5t) \\ \tau_{dr} = 0.2\cos(0.3t) \end{cases} \tag{38}$$

TABLE 1. Model parameters of AUV.

Index	Parameters	Value
1	$m(\mathrm{kg})$	33.68
2	$L(\mathrm{m})$	1.71
3	$z_g(\mathrm{m})$	0.02
4	$G(\mathrm{N})$	347.9
5	$X_u(\mathrm{kg/s})$	-8.105
6	$Y_v(\mathrm{kg/s})$	-62.025
7	$Z_w(\mathrm{kg/s})$	-61.701
8	$M_q(\mathrm{kg\cdot m^2/(rad\cdot s)})$	-42.637
9	$N_r(\mathrm{kg\cdot m^2/(rad\cdot s)})$	-48.776
10	$X_{\dot{u}}(\mathrm{kg})$	-0.93
11	$Y_{\dot{v}}(\mathrm{kg})$	-35.5
12	$Z_{\dot{w}}(\mathrm{kg})$	-35.5
13	$M_{\dot{q}}(\mathrm{kg\cdot m^2/rad})$	-4.88
14	$N_{\dot{r}}(\mathrm{kg\cdot m^2/rad})$	-4.88
15	$X_{u\|u\|}(\mathrm{kg/m})$	-3.9
16	$Y_{v\|v\|}(\mathrm{kg/m})$	-131
17	$Z_{w\|w\|}(\mathrm{kg/m})$	-131
18	$M_{q\|q\|}(\mathrm{kg\cdot m^2/rad^2})$	-188
19	$N_{r\|r\|}(\mathrm{kg\cdot m^2/rad^2})$	-94
20	$I_{yy}(\mathrm{kg\cdot m^2})$	3.54
21	$I_{zz}(\mathrm{kg\cdot m^2})$	3.54

The following results for Case 1 are shown in Fig. 5. Among them, Fig. 5a shows the following of the underactuated underwater robot in 3D space, while Figs. 5b and 5c show the following in two projection planes, respectively. It can be observed that by employing all four methods, the AUV can eventually converge to the desired path and move along the path, but there are differences in their following performance. In order to show the performance of the four methods more clearly, the positional following errors are compared, as shown in Fig. 6. It can be seen that the proposed method has almost no following error, while the following errors of the other three methods are relatively large, especially the most significant error of method 2. The expected angle following is shown in Fig. 7 and Fig. 8, and it can be clearly observed that the current actual heading of each method conforms to the expected heading, therefore, all the four methods can achieve good following, but the shapes of the expected angle curves are different, which mainly

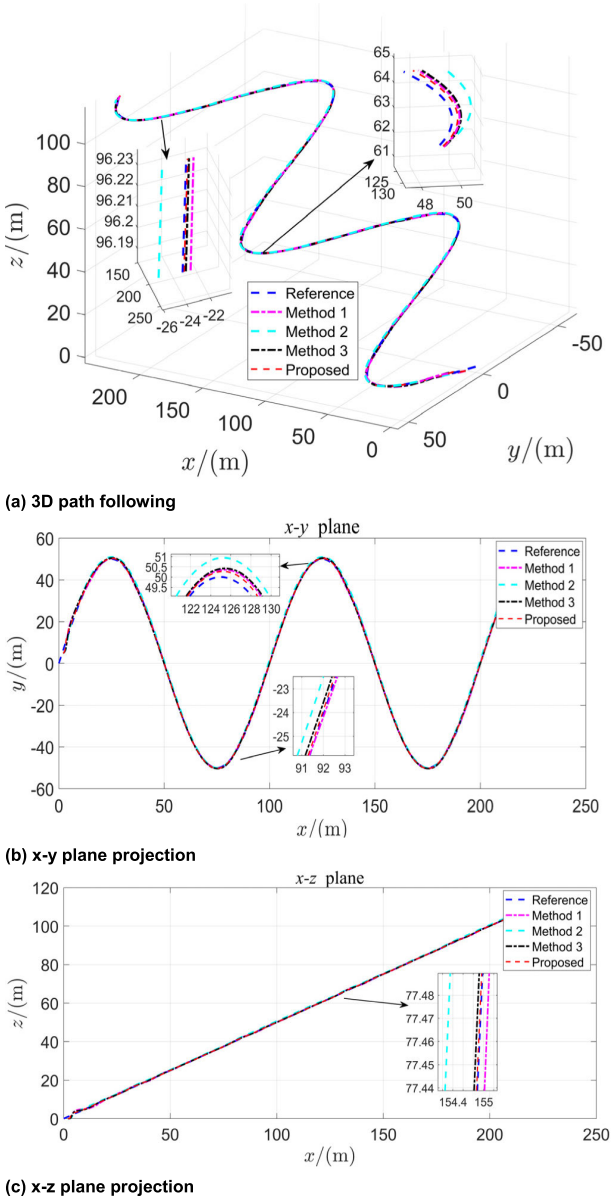

(a) 3D path following

(b) x-y plane projection

(c) x-z plane projection

FIGURE 5. Path following in case 1.

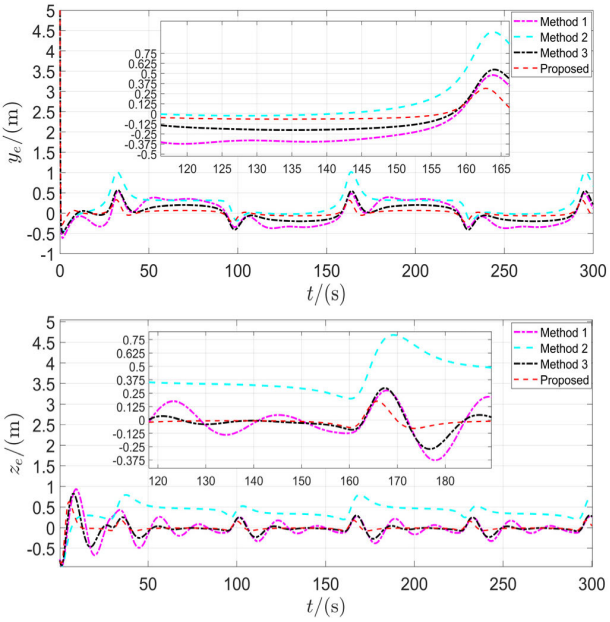

FIGURE 6. Position following error in case 1.

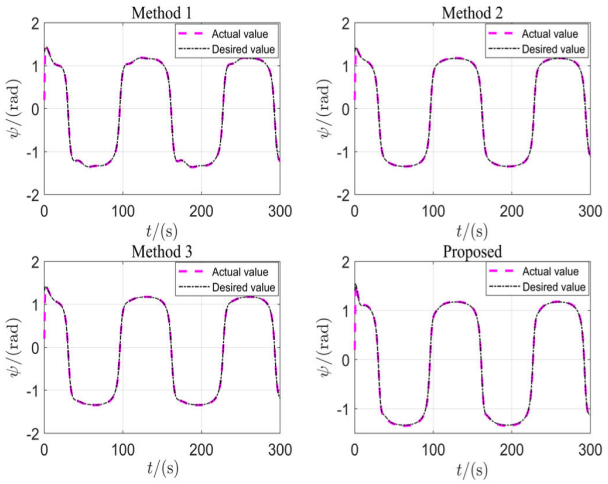

FIGURE 7. Heading angle following situation in case 1.

depends on the design of the guidance law, and the final following performance also mainly depends on the design of the guidance law. Fig. 9 demonstrates the estimation of angle of attack and crab angle under the two methods of ALOS and ILOS, and it can be seen that both methods can realize the estimation of the angle of attack and crab angle better, but the estimation result of ALOS has less fluctuation of deviation and better results. By comparing the velocities in Fig. 10 and Fig. 11, a similar conclusion can be drawn that the proposed method has less fluctuation and smooth velocity changes.

The error quantization results in Tab. 2 show that the proposed method performs the best, while Method 2 has the worst following accuracy and stability, and Method 3 performs closer to the proposed method. In addition, Fig. 12 demonstrates the estimation of the uncertainty disturbance and it is observed that the proposed nonlinear disturbance observer is able to estimate the disturbance variations well.

From the above analysis, the following conclusions can be drawn: compared with Method 1, the proposed method introduces a disturbance observer, which leads to better following control accuracy and robustness; compared with Method 2, the proposed method adds adaptive estimation laws for angle of attack and crab angle, which significantly improves the stability and accuracy of the controller; compared with Method 3, the adaptive results of the line-of-sight angle are better than the integral compensation under the simulation conditions results, so the proposed method has better following performance.

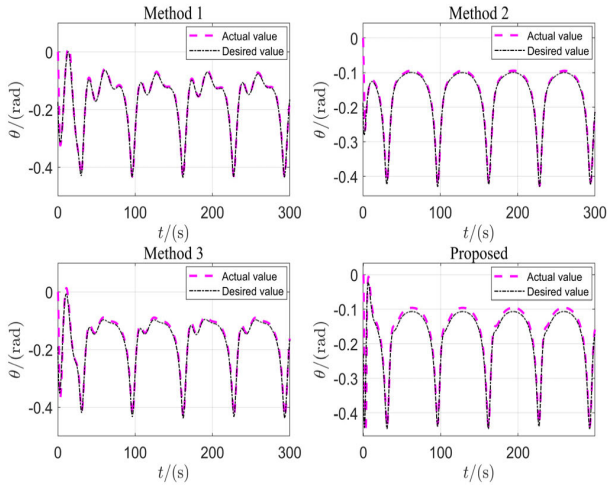

FIGURE 8. Pitch angle following situation in case 1.

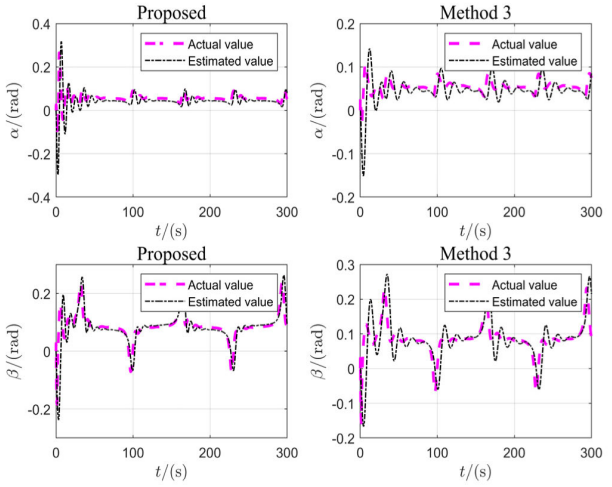

FIGURE 9. Angle estimation situation in case 1.

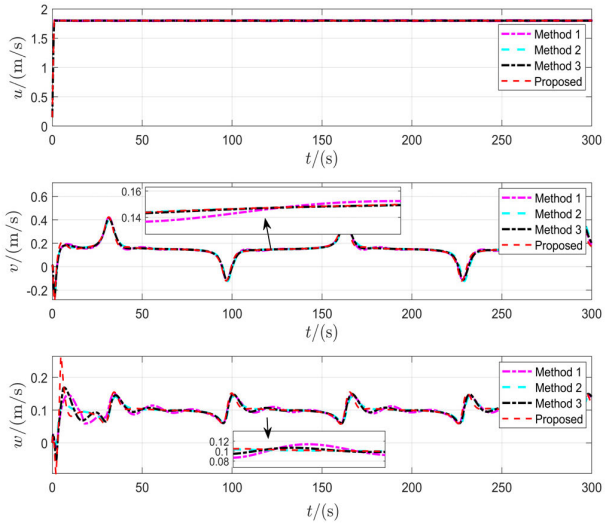

FIGURE 10. Comparison of line speeds in case 1.

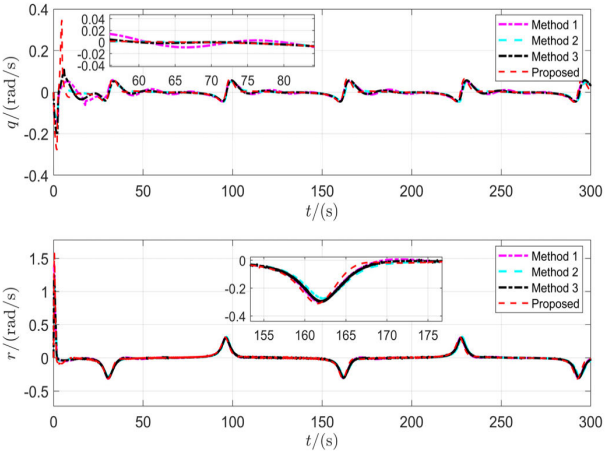

FIGURE 11. Comparison of angular velocities in case 1.

B. CASE 2: COMPARATIVE ANALYSIS OF PATH FOLLOWING IN TIME-VARYING CURRENTS AND DISTURBED ENVIRONMENTS

In order to further validate the performance and robustness of the proposed method for path following in complex time-varying currents and perturbation environments, a detailed simulation study is conducted in this case. For effective comparison, we choose the same desired path and initial conditions as in Case 1. Specifically, we consider time-varying, segmented currents and perturbations, which are:

$$u_{cx} = \begin{cases} 0.2\sin(0.3t) & t < 100s \\ 0.3\cos(0.5t) & 100\text{s} \le t < 200s \\ 0.15\cos(0.1t) & 200\text{s} \le t \end{cases}$$

$$v_{cy} = \begin{cases} 0.1\cos(0.1t) & t < 100s \\ 0.2\sin(0.3t) & 100\text{s} \le t < 200s \\ 0.15\cos(0.15t) & 200\text{s} \le t \end{cases} \quad (39)$$

$$w_{cz} = \begin{cases} 0.15\sin(0.15t) & t < 100s \\ 0.1\cos(0.3t) & 100\text{s} \le t < 200s \\ 0.15\sin(0.1t) & 200\text{s} \le t \end{cases}$$

$$\tau_{du} = \begin{cases} 0.7\sin(0.2t) & t < 100s \\ 0.3\cos(0.5t) & 100\text{s} \le t < 200s \\ 0.5\cos(0.3t) & 200\text{s} \le t \end{cases}$$

$$\tau_{dq} = \begin{cases} 0.2\sin(0.3t) & t < 100s \\ 0.6\cos(0.5t) & 100\text{s} \le t < 200s \\ 0.4\sin(0.1t) & 200\text{s} \le t \end{cases}$$

$$\tau_{dr} = \begin{cases} 0.25\sin(0.2t) & t < 100s \\ 0.35\sin(0.3t) & 100\text{s} \le t < 200s \\ 0.5\cos(0.5t) & 200\text{s} \le t \end{cases} \quad (40)$$

In Case 2, the details of the following situations are shown in Fig. 13 to Fig. 16, and the results of the error quantification are given in Table 3. The comprehensive analysis

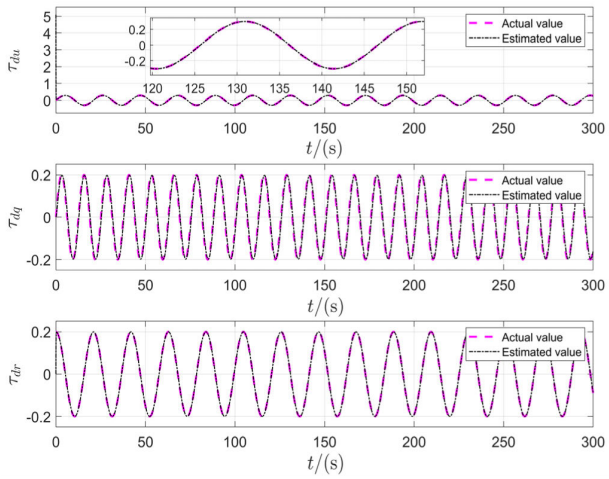

FIGURE 12. Disturbance estimation situation in case 1.

TABLE 2. Quantitative results of following performance for Case 1.

	Indicator	Method 1	Method 2	Method 3	proposed
y_e	MAE(m)	0.2723	0.2726	0.1848	0.0753
	RMSE(m)	0.3117	0.3882	0.2431	0.1460
z_e	MAE(m)	0.1659	0.4080	0.0992	0.0502
	RMSE(m)	0.2346	0.4328	0.1711	0.1029

TABLE 3. Quantitative results of following performance for Case 2.

	Indicator	Method 1	Method 2	Method 3	Proposed
y_e	MAE(m)	0.3297	0.2697	0.2004	0.0758
	RMSE(m)	0.3880	0.3518	0.2552	0.1381
z_e	MAE(m)	0.4310	0.2973	0.2089	0.0834
	RMSE(m)	0.5055	0.3478	0.2685	0.1396

shows that the proposed method has better following accuracy and stability compared to the other three methods. In the face of time-varying currents and perturbations, the proposed method exhibits smaller fluctuations in the position following error, while the other three methods show obvious oscillations. In addition, according to the quantitative data in Table 2, the error increase of the proposed method under time-varying currents and disturbances is significantly smaller than that of the other three methods, which reflects the better adaptability and robustness of our method in complex environments. By comparing the velocity changes in Fig. 15 and Fig. 16, it can be observed that Methods I and III oscillate when the current frequency increases, while the proposed method fluctuates less.

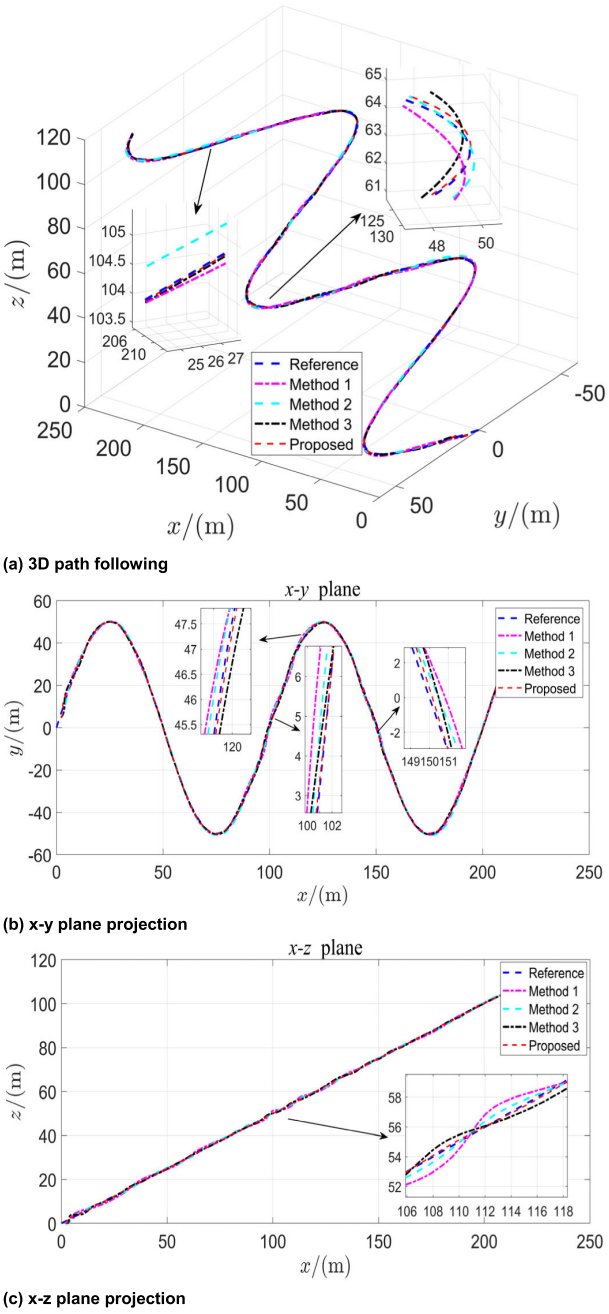

(a) 3D path following

(b) x-y plane projection

(c) x-z plane projection

FIGURE 13. Path following in case 2.

Fig. 17 demonstrates the results of angle of attack and crab angle estimation in time-varying currents and disturbed environments. It can be observed that compared to the ILOS method, the proposed ALOS method has smaller estimation bias and significantly lower hysteresis when facing time-varying currents, showing higher accuracy. By comparing with Case 1, it can be more clearly illustrated that the effect distinction between the two estimation methods becomes more obvious as the ocean current increases. The estimation results of the disturbances are shown in Fig. 18, where it can also be observed that the proposed nonlinear disturbance observer is able to estimate the uncertainties well, and even

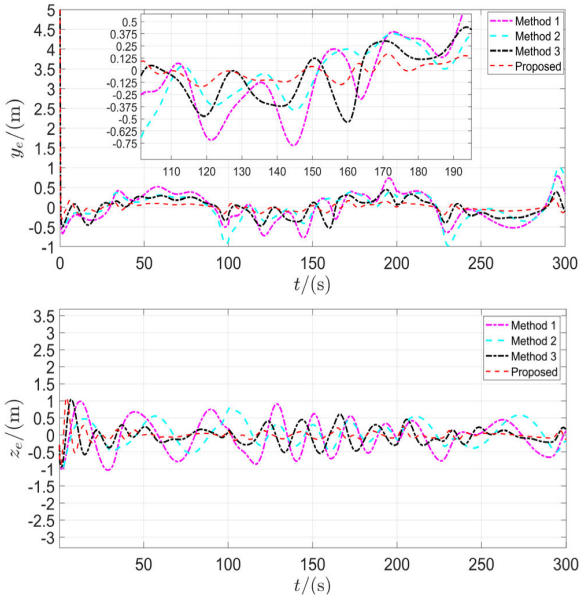

FIGURE 14. Position following error in case 2.

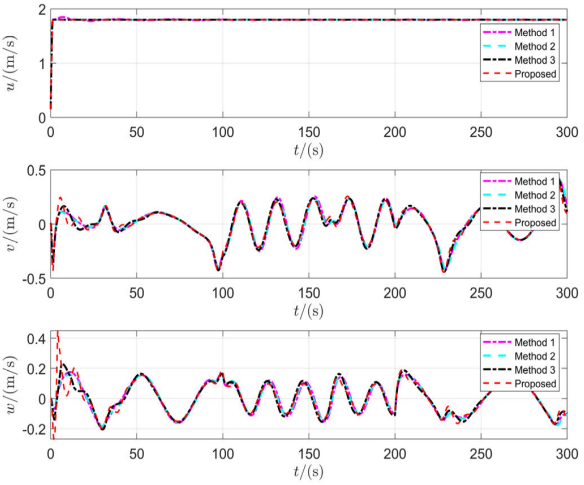

FIGURE 15. Comparison of line speeds in case 2.

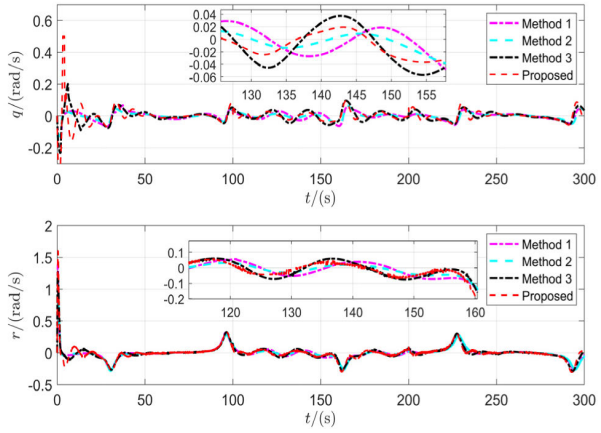

FIGURE 16. Comparison of angular velocities in case 2.

though the actual values of the disturbances show large breaks at 100 and 200 s, the estimates following this point still track the actual values well.

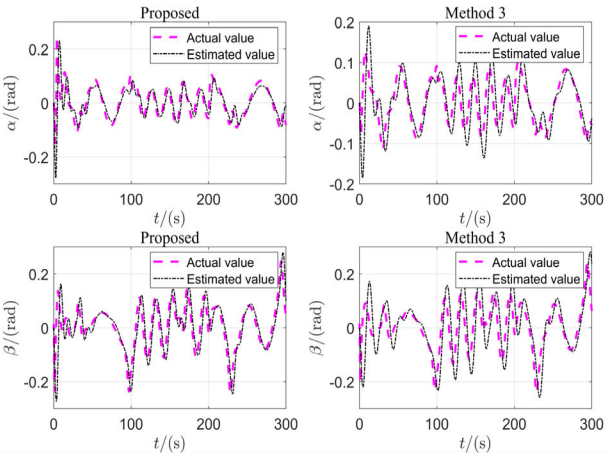

FIGURE 17. Comparison of angular velocities in case 2.

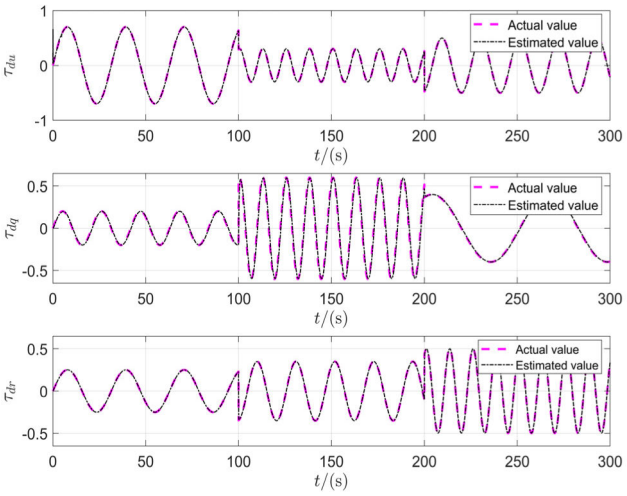

FIGURE 18. Disturbance estimation situation in case 2.

In summary, based on the validation of Case 1 and Case 2, the proposed control method shows good following performance and robustness in different environments. Compared to Method I, the proposed method has better following stability, indicating that the NDO-based controller has better control and resistance in the face of disturbances. The proposed method has better following accuracy compared to methods II and III. The LOS guidance law used in Method II always causes the navigator to deviate from the desired path, and Method III has a degraded performance in the face of rapidly changing angle of attack and crab angle.

V. CONCLUSION

A new backstepping sliding mode control method combining a nonlinear disturbance observer and an adaptive line-of-sight braking law is proposed for the 3D path following control problem of an underactuated AUV under multiple uncertainties such as sea currents and unknown disturbances. The adaptive line-of-sight guidance law is designed for time-varying currents to compensate for the sideslip and the angle of attack, and the nonlinear disturbance observer

is designed to estimate the composite disturbances of the system, while the sliding-mode control term is introduced to further enhance the robustness of the system to the uncertain disturbances. The good performance and strong robustness of the proposed method in 3D path following control are verified through numerical simulations. The superiority of the proposed control scheme over other similar methods is further confirmed by quantitative error analysis.

In the field of underwater path following, achieving precise positioning is a major challenge, mainly due to the complexity of the underwater environment. Inertial navigation systems, although excellent in terms of independence and accuracy, encounter the problem of error accumulation in long-term operation. Meanwhile, hydroacoustic navigation systems, while providing highly accurate positioning information, are limited by cost and underwater acoustic conditions.

In order to enhance the robustness of the system and improve positioning accuracy, it is planned to integrate a variety of assisted navigation technologies. The visual navigation system will utilize cameras and image processing techniques to obtain visual information about the environment, while the magnetic navigation system will assist positioning through changes in the Earth's magnetic field. Underwater terrain matching navigation technology is also being actively explored to enhance the accuracy and robustness of navigation to meet the needs of future experiments. Currently, our AUV is small in size and carries a domestic MEMS inertial navigation system. Nevertheless, we aim to verify the correctness of the theory through theoretical contributions and practical tests, and make progress in the field of underwater path following. The focus of future work will be to conduct a large number of experiments in open water to verify the effectiveness of the proposed control algorithm and to gradually solve the challenges posed by harsh and complex marine environments.

REFERENCES

[1] R. B. Wynn, V. A. I. Huvenne, T. P. Le Bas, B. J. Murton, D. P. Connelly, B. J. Bett, H. A. Ruhl, K. J. Morris, J. Peakall, D. R. Parsons, E. J. Sumner, S. E. Darby, R. M. Dorrell, and J. E. Hunt, "Autonomous underwater vehicles (AUVs): Their past, present and future contributions to the advancement of marine geoscience," *Mar. Geol.*, vol. 352, pp. 451–468, Jun. 2014, doi: 10.1016/j.margeo.2014.03.012.

[2] R. Salazar, A. Campos, V. Fuentes, and A. Abdelkefi, "A review on the modeling, materials, and actuators of aquatic unmanned vehicles," *Ocean Eng.*, vol. 172, pp. 257–285, Jan. 2019, doi: 10.1016/j.oceaneng.2018.11.047.

[3] Z. Chen, W. Jiao, K. Ren, J. Yu, Y. Tian, K. Chen, and X. Zhang, "A survey of research status on the environmental adaptation technologies for marine robots," *Ocean Eng.*, vol. 286, Oct. 2023, Art. no. 115650, doi: 10.1016/j.oceaneng.2023.115650.

[4] X. Xiang, C. Yu, L. Lapierre, J. Zhang, and Q. Zhang, "Survey on fuzzy-logic-based guidance and control of marine surface vehicles and underwater vehicles," *Int. J. Fuzzy Syst.*, vol. 20, no. 2, pp. 572–586, Feb. 2018, doi: 10.1007/s40815-017-0401-3.

[5] T. I. Fossen and A. M. Lekkas, "Direct and indirect adaptive integral line-of-sight path-following controllers for marine craft exposed to ocean currents," *Int. J. Adapt. Control Signal Process.*, vol. 31, no. 4, pp. 445–463, Apr. 2017, doi: 10.1002/acs.2550.

[6] T. I. Fossen, M. Breivik, and R. Skjetne, "Line-of-sight path following of underactuated marine craft," *IFAC Proc. Volumes*, vol. 36, no. 21, pp. 211–216, Sep. 2003, doi: 10.1016/s1474-6670(17)37809-6.

[7] M. Breivik and T. I. Fossen, "Path following for marine surface vessels," in *Proc. Techno-Ocean*, vol. 4, Nov. 2004, pp. 2282–2289, doi: 10.1109/OCEANS.2004.1406507.

[8] M. Breivik and T. I. Fossen, "Guidance laws for autonomous underwater vehicles," Ph.D. dissertation, Dept. Naval Archit. Ocean Eng., NTNU, I-Tech, Vienna, Austria, 2009, doi: 10.5772/6696.

[9] E. Borhaug, A. Pavlov, and K. Y. Pettersen, "Integral LOS control for path following of underactuated marine surface vessels in the presence of constant ocean currents," in *Proc. 47th IEEE Conf. Decis. Control*, 2008, pp. 4984–4991.

[10] W. Caharija, M. Candeloro, K. Y. Pettersen, and A. J. Sørensen, "Relative velocity control and integral LOS for path following of underactuated surface vessels," *IFAC Proc. Volumes*, vol. 45, no. 27, pp. 380–385, Apr. 2012, doi: 10.3182/20120919-3-it-2046.00065.

[11] W. Caharija, K. Y. Pettersen, M. Bibuli, P. Calado, E. Zereik, J. Braga, J. T. Gravdahl, A. J. Sørensen, M. Milovanovic, and G. Bruzzone, "Integral line-of-sight guidance and control of underactuated marine vehicles: Theory, simulations, and experiments," *IEEE Trans. Control Syst. Technol.*, vol. 24, no. 5, pp. 1623–1642, Sep. 2016, doi: 10.1109/TCST.2015.2504838.

[12] T. I. Fossen, K. Y. Pettersen, and R. Galeazzi, "Line-of-sight path following for Dubins paths with adaptive sideslip compensation of drift forces," *IEEE Trans. Control Syst. Technol.*, vol. 23, no. 2, pp. 820–827, Mar. 2015, doi: 10.1109/TCST.2014.2338354.

[13] X. Yao, "Control for 3D path-following of underactuated autonomous underwater vehicle under current disturbance," *J. Harbin Inst. Technol.*, vol. 51, no. 3, pp. 37–45, Apr. 2019, doi: 10.11918/j.issn.0367-6234.201709002.

[14] L. Liu, D. Wang, and Z. Peng, "ESO-based line-of-sight guidance law for path following of underactuated marine surface vehicles with exact sideslip compensation," *IEEE J. Ocean. Eng.*, vol. 42, no. 2, pp. 477–487, Apr. 2017, doi: 10.1109/JOE.2016.2569218.

[15] Y. Xia, K. Xu, Y. Li, G. Xu, and X. Xiang, "Improved line-of-sight trajectory tracking control of under-actuated AUV subjects to ocean currents and input saturation," *Ocean Eng.*, vol. 174, pp. 14–30, Feb. 2019, doi: 10.1016/j.oceaneng.2019.01.025.

[16] C. Yu, C. Liu, L. Lian, X. Xiang, and Z. Zeng, "ELOS-based path following control for underactuated surface vehicles with actuator dynamics," *Ocean Eng.*, vol. 187, Sep. 2019, Art. no. 106139, doi: 10.1016/j.oceaneng.2019.106139.

[17] P. Du, W. Yang, Y. Chen, and S. H. Huang, "Improved indirect adaptive line-of-sight guidance law for path following of underactuated AUV subject to big ocean currents," *Ocean Eng.*, vol. 281, Aug. 2023, Art. no. 114729, doi: 10.1016/j.oceaneng.2023.114729.

[18] F. Liu, Y. Shen, B. He, D. Wang, J. Wan, Q. Sha, and P. Qin, "Drift angle compensation-based adaptive line-of-sight path following for autonomous underwater vehicle," *Appl. Ocean Res.*, vol. 93, Dec. 2019, Art. no. 101943, doi: 10.1016/j.apor.2019.101943.

[19] T. I. Fossen, "An adaptive line-of-sight (ALOS) guidance law for path following of aircraft and marine craft," *IEEE Trans. Control Syst. Technol.*, vol. 31, no. 6, pp. 2887–2894, Nov. 2023, doi: 10.1109/TCST.2023.3259819.

[20] M. W. Hasan and N. H. Abbas, "Disturbance rejection for underwater robotic vehicle based on adaptive fuzzy with nonlinear PID controller," *ISA Trans.*, vol. 130, pp. 360–376, Nov. 2022, doi: 10.1016/j.isatra.2022.03.020.

[21] B. M. Patre, P. S. Londhe, L. M. Waghmare, and S. Mohan, "Disturbance estimator based non-singular fast fuzzy terminal sliding mode control of an autonomous underwater vehicle," *Ocean Eng.*, vol. 159, pp. 372–387, Jul. 2018, doi: 10.1016/j.oceaneng.2018.03.082.

[22] C. Yuan, "Adaptive optimal 3D nonlinear compound line-of-sight trajectory following control for over-actuated AUVs in attitude space," *Ocean Eng.*, vol. 274, no. 15, Apr. 2023, Art. no. 114056, doi: 10.1016/j.oceaneng.2023.114056.

[23] S. Rong, H. Wang, H. Li, W. Sun, Q. Gu, and J. Lei, "Performance-guaranteed fractional-order sliding mode control for underactuated autonomous underwater vehicle trajectory tracking with a disturbance observer," *Ocean Eng.*, vol. 263, Nov. 2022, Art. no. 112330, doi: 10.1016/j.oceaneng.2022.112330.

[24] Q. Zhu, H. Shang, X. Lu, and Y. Chen, "Adaptive sliding mode tracking control of underwater vehicle-manipulator systems considering dynamic disturbance," *Ocean Eng.*, vol. 291, Jan. 2024, Art. no. 116300, doi: 10.1016/j.oceaneng.2023.116300.
[25] Z. Peng, J. Wang, and J. Wang, "Constrained control of autonomous underwater vehicles based on command optimization and disturbance estimation," *IEEE Trans. Ind. Electron.*, vol. 66, no. 5, pp. 3627–3635, May 2019, doi: 10.1109/TIE.2018.2856180.
[26] C. Ma, J. Jia, T. Zhang, S. Wu, and D. Jiang, "Horizontal trajectory tracking control for underactuated autonomous underwater vehicles based on contraction theory," *J. Mar. Sci. Eng.*, vol. 11, no. 4, p. 805, Apr. 2023, doi: 10.3390/jmse11040805.
[27] X. Yang, X. Zhu, W. Liu, H. Ye, W. Xue, C. Yan, and W. Xu, "A hybrid autonomous recovery scheme for AUV based Dubins path and non-singular terminal sliding mode control method," *IEEE Access*, vol. 10, pp. 61265–61276, 2022, doi: 10.1109/ACCESS.2022.3180836.
[28] J. Zhang, X. Xiang, W. Li, and Q. Zhang, "Adaptive saturated path following control of underactuated AUV with unmodeled dynamics and unknown actuator hysteresis," *IEEE Trans. Syst. Man Cybern., Syst.*, vol. 53, no. 10, pp. 6018–6030, Oct. 2023, doi: 10.1109/TSMC.2023.3280065.
[29] X. Xiang, C. Yu, and Q. Zhang, "Robust fuzzy 3D path following for autonomous underwater vehicle subject to uncertainties," *Comput. Operations Res.*, vol. 84, pp. 165–177, Aug. 2017, doi: 10.1016/j.cor.2016.09.017.
[30] E. Peymani and T. I. Fossen, "Path following of underwater robots using Lagrange multipliers," *Robot. Auto. Syst.*, vol. 67, pp. 44–52, May 2015, doi: 10.1016/j.robot.2014.10.011.
[31] X. Wang, "Motion control and path planning research for underactuated autonomous underwater vehicle," Ph.D. dissertation, Dept. Naval Archit. Ocean Eng., Harbin Eng. Univ., Harbin, Heilongjiang, China, 2020.
[32] M. Breivik and T. I. Fossen, "A unified control concept for autonomous underwater vehicles," in *Proc. Amer. Control Conf.*, Minneapolis, MN, USA, 2006, p. 7, doi: 10.1109/acc.2006.1657500.
[33] K. D. Do, J. Pan, and Z. P. Jiang, "Robust and adaptive path following for underactuated autonomous underwater vehicles," *Ocean Eng.*, vol. 31, no. 16, pp. 1967–1997, Nov. 2004, doi: 10.1016/j.oceaneng.2004.04.006.
[34] A. P. Aguiar and J. P. Hespanha, "Trajectory-tracking and path-following of underactuated autonomous vehicles with parametric modeling uncertainty," *IEEE Trans. Autom. Control*, vol. 52, no. 8, pp. 1362–1379, Aug. 2007, doi: 10.1109/TAC.2007.902731.
[35] N. Fischer, D. Hughes, P. Walters, E. M. Schwartz, and W. E. Dixon, "Nonlinear RISE-based control of an autonomous underwater vehicle," *IEEE Trans. Robot.*, vol. 30, no. 4, pp. 845–852, Aug. 2014, doi: 10.1109/TRO.2014.2305791.
[36] X. Xiang, "Research on path following and coordinated control for second-order nonholonomic AUVs," Ph.D. dissertation, Dept. Naval Archit. Ocean Eng., Huazhong Univ. Sci., China, 2010.
[37] W. Chen, "Adaptive backstepping control of underactuated AUV based on disturbance observer," *J. Central South Univ. Sci. Technol.*, vol. 48, no. 1, pp. 69–76, Jan. 2017, doi: 10.11817/j.issn.1672-7207.2017.01.010.
[38] S. An, L. Wang, and Y. He, "Robust fixed-time tracking control for underactuated AUVs based on fixed-time disturbance observer," *Ocean Eng.*, vol. 266, Dec. 2022, Art. no. 112567, doi: 10.1016/j.oceaneng.2022.112567.
[39] W. Luo and S. Liu, "Disturbance observer based nonsingular fast terminal sliding mode control of underactuated AUV," *Ocean Eng.*, vol. 279, Jul. 2023, Art. no. 114553, doi: 10.1016/j.oceaneng.2023.114553.
[40] L. He, "Hydrodynamic profile optimization of AUV based on response surface method," *J. Ordn. Equip. Eng.*, vol. 43, no. 12, pp. 43–50, Dec. 2022, doi: 10.11809/bqzbgcxb2022.12.007.

LONG HE was born in Hebei, China, in 1998. He is currently pursuing the Ph.D. degree in weapon science and technology with the College of Mechatronic Engineering, North University of China. His research interests include motion control and formation coordination of AUVs.

YA ZHANG is currently a Professor and a Ph.D. Supervisor with the North University of China. He is responsible for arranging experimental resources and providing comprehensive guidance for conducting field experiments and numerical analysis. His research interests include the overall design of robots and the control of nonlinear systems.

GANG FAN was born in 1989. He is currently pursuing the Ph.D. degree with the College of Mechatronic Engineering, North University of China. His main research interests include underwater positioning and navigation technology, deep learning, and machine learning.

YANG LIU was born in 1994. He received the B.S. degree in electrical and mechanical engineering from Shijiazhuang Tiedao University, in 2018. He is currently pursuing the Ph.D. degree with the School of Electromechanical Engineering, North University of China. His main research interests include underwater localization, acoustic signal processing, and target tracking.

XUE WANG was born in 1989. She received the master's degree from the North University of China, in 2016, where she is currently pursuing the Ph.D. degree. Her research interests include artificial intelligence and electromechanical systems.

ZEHUI YUAN was born in 1985. She received the B.Sc. degree in mechatronics engineering from Northeastern University, China, in 2007, the M.Sc. degree in mechatronics engineering from Harbin Institute of Technology, China, in 2009, and the Ph.D. degree in mechatronics engineering from the Politecnico di Torino, Italy, in 2013. In 2014, she joined the North University of China, Taiyuan, China, where she is teaching signal processing and robotic courses. Her research interests include computer vision applied to robot localization and mapping, guidance, and the control of autonomous vehicles.